A Multiplexing Ripple Cancellation LED Driver with True Single-Stage Power Conversion and Flicker-free Operation

Peng Fang
Department of Electrical Engineering
University of Minnesota
Duluth, USA
fangp@d.umn.edu

Yan-Fei, Liu, Paresh C. Sen
Department of Electrical and Computer Engineering
Queen's University
Kingston, Canada
yanfeiliu@queensu.ca, senp@queensu.ca

Abstract—**although a single-stage off-line power LED driver can achieve low cost and high efficiency, the notorious double-line-frequency flicker issue with a single-stage LED driver limits its usage in high-quality lighting applications. To solve lighting flicker, as well as maintain a low cost and high efficiency, a Multiplexing Ripple Cancellation (MRC) LED driver is proposed in this paper. One switching cycle is divided into two intervals. During the first interval, the proposed LED driver operates as a conventional LED driver that transfers energy from AC input to LED output, performs power factor correction and generates the main output voltage. The main output voltage has a double-line-frequency ripple like in a conventional design. During the second interval, the proposed LED driver transfers energy from AC input again to generate an opposite ripple voltage to cancel the ripple voltage from the main output. In this way, the voltage across LED load is a DC to achieve flicker-free LED driving performance. More than 99% of the output power goes through one-time power conversion while less than 1% goes through two-time power conversion. A 7.5W experimental prototype had been built and tested to verify the design concept.**

Keywords—Single stage, ripple cancellation, flick-free operation, multiplexing operation,

I. INTRODUCTION

The light-emitting diode (LED) offers much higher efficacy than any other lighting devices and is one of the most promising lighting technologies. High quality LED light devices are more durable and provide comparable, if not better, light quality as other types of lighting. It has the potential to completely overtake other traditional light technologies, especially in residential applications. The global LED lighting market reached 26 billion U.S dollar in 2016 and is expected to reach 54 Billion U.S dollar by 2022, growing at a rate of around 13% between 2017 and 2022 [1].

A variety of research had been conducted to maintain a low cost, and higher efficiency as a single-stage LED driver while achieving flicker-free operation as a two-stage LED driver. The energy buffering technologies [4]-[7] had been proposed to balance energy difference between AC input and LED output with a bi-directional DC-DC converter. The two-stage integrated methods [8]-[11] had been proposed to share components between the first PFC stage and the second DC-DC stage, which can reduce component cost. The harmonic input currents injection method [12]-[14] had been proposed to minimize double-line-frequency imbalanced energy existing in a single-stage LED driver. Therefore, the ripple LED current is reduced to alleviate lighting flicker. The ripple cancellation method had been proposed in [15]-[20] to achieve flicker-free LED driving performance. The

energy channeling LED driver is proposed in [20]. One limitation with the energy channeling LED driver is restrained operation. The input power drop to zero as the result of performing power factor correction. The input power is not enough to maintain the ripple cancellation voltage during the input is close to zero. A Multiplexing Ripple Cancellation (MRC) LED driver is proposed in this paper. The way to generate the ripple cancellation voltage is made independent of the power factor correction operation, which removes the restraint of having limited input power to maintain the ripple cancellation voltage during the input voltage zero-crossing.

This remaining of this paper is organized as follows. Section II discusses the concept and operating principle of the proposed LED driver; Section III discusses the control strategy of the LED driver; Section IV discusses the design consideration of the proposed LED driver. The experimental result of the proposed LED driver is presented in section V. Finally, the paper is concluded at section VI.
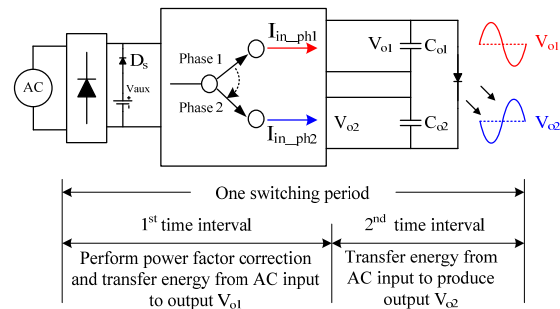

Fig. 1 Concept of the proposed multiplexing ripple cancellation LED driver

II. CONCEPT AND OPERATING PRINCIPLE

Fig. 1 shows the operation concept of the proposed MRC LED driver. It operates in time multiplexing manner with one switching cycle being divided into two intervals, namely, the interval I and the interval II. During the time interval I, the power stage of the conceptual LED driver operates as a PFC converter. Energy is transferred from AC input to the main output V_{o1} and power factor correction is performed. During the interval II, it operates as a ripple cancellation converter. The energy used to maintain V_{o2} is also from the AC input. The energy transferred from AC input to both output V_{o1} and V_{o2} is in single-stage power conversion manner, which helps maintain a comparable high efficiency as a conventional single-stage LED driver. Fig. 2 shows a Buck-Boost topology based implementation of the MRC

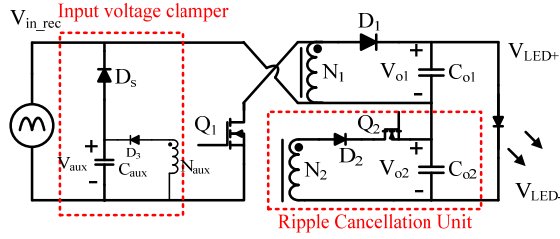LED driver. Fig. 3 shows one switching cycle operation of the MRC LED driver.

Fig. 2 Circuit implementation of the MRC LED driver based on Buck-Boost topology

The critical switching waveforms in one switching cycle are shown in Fig. 4. The following brief analysis explains how power factor correction is performed during time interval I operation. The switching current starts from zero at the beginning of the time interval I operation. The on time of the interval I operation, $[t_0\text{-}t_1]$, is a constant in a half line cycle. The interval II operation will not start until the switching current, I_{D1}, drops to zero. At the end of time interval II operation, switching current I_{D2} also drop to zero. The switching period is constant in every switching cycle. The detailed switching operation in each time interval will be discussed as follows.

During time interval [t₀-t1]

A switching cycle starts at time t_0 when the MOSFET Q_1 is turned on. The inductor is charged by the rectified AC input. The switching current, in winding N_1, starts rising from zero and increases linearly with the turn on time. The switching current in winding N_1 (and Q_1) peaks at time t1 right before Q_1 is turned off and can be expressed as:

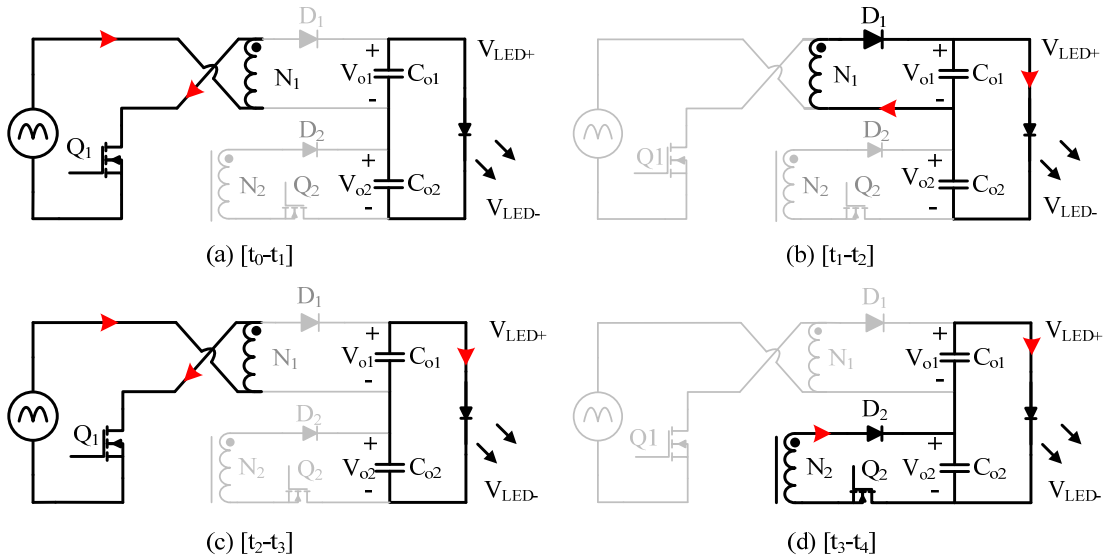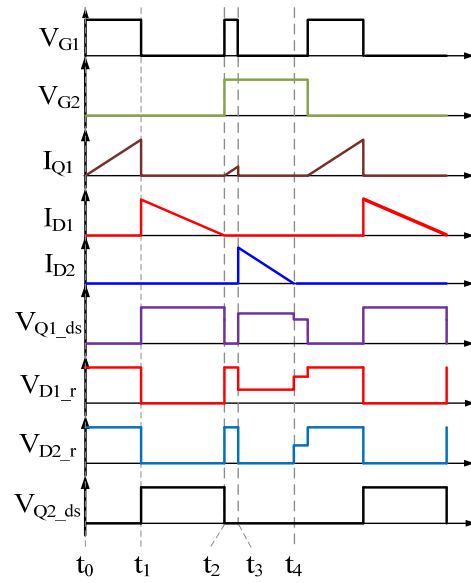$$I_{Q_1\_t_1} = \frac{V_{in} \times (t_1 - t_0)}{L_{N1}}$$ (1)

Fig. 4 Key switching current waveforms of the proposed MRC LED driver

The averaged current drawn from AC input during time interval I operation can be expressed as:

$$I_{in\_T1\_avg} = \frac{I_{Q1\_t_1} \times (t_1 - t_0)}{2T_s}$$ (2)

Where in (2), $I_{in\_T1\_avg}$ represents the averaged input current in a switching cycle during interval I operation. Further combining Eq. (1) and (2) yields:

(a) [t₀-t₁]

(b) [t₁-t₂]

(c) [t₂-t₃]

(d) [t₃-t₄]

Fig. 3 One switching cycle operation of the proposed multiplexing ripple cancellation LED driver

$$I_{in\_T1\_avg} = \frac{V_{in} \times (t_1 - t_0)^2}{2 \times T_s \times L_{N1}} \qquad (3)$$

As both the terms (t_1-t_0) and T_s are constant in a half line cycle, $I_{in\_T1\_avg}$ is therefore proportional to the input voltage. Because of the opposite winding orientation between N_1 and N_2, both diodes D_1, D_2 are reversely biased and there is no current in winding N_2. The body diode of the MOSFET Q_2 is forward biased. The voltage stresses on D_1 and D_2 during this time interval can be expressed as:

$$V_{D_1[t_0-t_1]} = V_{o1} + V_{in} \qquad (4)$$

$$V_{D_2[t_0-t_1]} = V_{o2} + V_{in} \times \frac{N_2}{N_1} \qquad (5)$$

During Time Interval [t_1-t_2]

As the MOSFET Q_1 is turned off at time t1, the magnetic current in winding N_1 is forced to conduct in diode D_1. The voltage across winding N_1 is clamped to be the same as the output Vo1 (ignoring the forward voltage drop of diode D_1). The voltage across MOSFET Q_1 is the sum of input voltage and output voltage V_{o1}, and is expressed as:

$$V_{Q_1[t_1-t_2]} = V_{in} + V_{o1} \qquad (6)$$

During this time interval, the energy stored in the inductor is transferred to the output V_{o1}. The magnetic current in winding N_1 starts decreasing at time t_1 and becomes zero at time t_2, which ends the interval I operation. One should note that, during this time interval, the voltage on winding N_2, $V_{N2}[t_1$-$t_2]$, is designed to be higher than V_{o2} as shown below:

$$V_{N_2[t_1-t_2]} = V_{o1} \times \frac{N_2}{N_1} > V_{o2} \qquad (7)$$

Therefore, the diode D_2 is forward biased while the body diode of Q_2 is reversely biased. The voltage across the drain to source terminals of Q_2 can be expressed as:

$$V_{Q_2[t_1-t_2]} = V_{N_2[t_1-t_2]} - V_{o2} = V_{o1} \times \frac{N_2}{N_1} - V_{o2} \qquad (8)$$

During Time Interval [t_2-t_3]

The time interval II operation starts at time t_2 and the MOSFET Q_1 is turned on again. The voltage stresses on these power components are the same as they are during the time interval [t_0-t_1]. The inductor current in MOSFET Q_1 peaks at t_3 again before Q_1 is turned off. The switching current in Q_1 at t_3 is expressed as:

$$I_{Q_1\_t_3} = \frac{V_{in} \times (t_3 - t_2)}{L_{N1}} \qquad (9)$$

The MOSFET Q_2 is designed to be turned on at t_2. Theoretically, the MOSFET Q_2 can be turned on anywhere within [t_2-t_3] without affecting the expected operation.

During Time Interval [t_3-t_4]

When the MOSFET Q_1 is turned off at t_3, the magnetic inductor current needs to find another path to continue the current flow. As Q_2 is already on, both winding N_1 and N_2 provide current flowing paths. The turns ratio N_1:N_2 in the proposed design forces the magnetic current to continue flowing in the winding N_2 and the explanation is as follows.

If the magnetic current conducts in winding N_2, the voltage across the winding N_2 is clamped at V_{o2} (with ignoring the forward voltage drop of D_2). The voltage reflected on the winding N_1 becomes:

$$V_{N_1[t_3-t_4]} = V_{o2} \times \frac{N_2}{N_1} \qquad (10)$$

Combining (14) and (17) yields:

$$V_{N_1[t_3-t_4]} < V_{o1} \qquad (11)$$

(18) Indicates that the voltage potential at the anode of D_1 is smaller than the voltage potential at the cathode of D_1. Therefore, the diode D_1 is reversely biased. Therefore, the above assumption is valid and the magnetic current only conducts in winding N_2 during [t_3-t_4]. The inductor releases the stored energy to the output V_{o2} during the time interval [t_3-t_4]. The magnetic current in winding N_2 starts decreasing from t_3 and it drops to zero at time t_4, which ends the time interval II operation. There is a voltage falling on the MOSFET Q_1 again, which can be expressed as:

$$V_{Q_1[t_3-t_4]} = V_{in} + V_{o2} \times \frac{N_1}{N_2} \qquad (12)$$

During Time Interval [t_4-t_5]

There is a small time interval [t_4-t_5] to maintain DCM operation. There is no active energy transfer during this time interval and the magnetic current in the inductor remains zero.

III. CONTROL SCHME

Fig. 5 shows the control diagram of the proposed Multiplex Ripple Cancellation LED driver. Two control loops are needed for the LED driver, namely the LED current feedback loop and the output V_{o2} voltage loop.
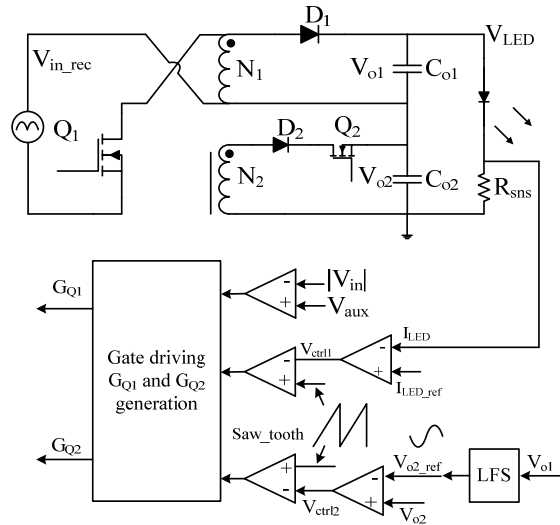

Fig. 5 Control diagram of the proposed MRC LED driver

To achieve LED current regulation, LED current is sensed and compared with its current reference. The compensated error signal, V_{ctrl1}, is compared with the saw-tooth signal to generate the gate driving signal for the

MOSFET Q_1 during the interval I operation. Under steady state, Vctrl1 is a constant in a half line cycle. Therefore, the on time of Q_1 during phase one, (t_1-t_0), is constant. Under discontinuous conduction mode and Flyback topology, the interval I input current automatically follows the input voltage to perform the power factor correction [33]. When the sensed input current is not equal to the LED current reference, V_{ctrl1} will be changed automatically by the feedback loop. Therefore, (t_1-t_0) and the RMS input current will change. The change with RMS input current lead to change of the input power and the output voltage V_{o1}. V_{o1} will settle to the value that produce exact the LED current required by its reference. It should note that the averaged voltage of V_{o2} is a constant, and it is not a part of the LED current regulation loop.

To achieve ripple cancellation, the output voltage V_{o1} is sensed by the low-frequency sensing (LFS) circuit to extract the double-line-frequency ripple voltage. The sensed ripple voltage becomes the reference voltage of V_{o2}, V_{o2_ref}. The output voltage V_{o2} is sensed and compared with this reference. The compensated error voltage Vctrl2 is compared with the saw tooth signal to produce the gate driving signal of Q_1 during the interval II operation. With a well-controlled regulation loop, the output V_{o2} tightly follows the reference voltage and produce an opposite ripple voltage to cancel the ripple from V_{o1}. There is also another logic that controls the gate driving of Q_1. When $|V_{in}| < V_{aux}$, the gate driving of Q_1 during interval I operation is disabled. In this way, no energy is delivered to the output V_{o1} during this period, minimizing the amount of energy going through two times power conversion.

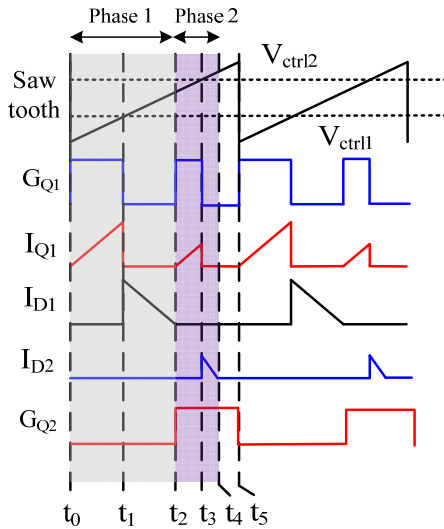Fig. 6 shows how to generate the gate driving signals for Q_1 and Q_2.

Fig. 6 Gate driving generating scheme for Q_1 and Q_2

IV. DESIGN CONSIDERATIONS

EnergyStar requires power factor implementation for LED drivers with greater than 5W output. In the proposed design, the interval II input current introduces distortion, which inevitably affects the power factor performance. A model to simulate the average input current of the proposed

LED driver has been built. The power factor performance simulation is based on 110Vrms input, and the results are shown in TABLE 1. To normalize the result, the voltage ripple of V_{o1} is presented as the ratio of V_{o1_rip} / V_{LED}, where V_{o1_rip} is the ripple voltage amplitude of V_{o1}. Please note, the DC amplitude of V_{o2}, V_{o2_DC}, is designed based on the minimum requirement to be just enough to maintain V_{o2} above zero. Therefore, in the proposed design, there is $V_{o2\_DC} = V_{o1\_rip} = V_{o2\_rip}$. In this way, the averaged power delivered to the V_{o2} is minimized and so is the input current distortion. In a real design, V_{o2_DC} can be designed slightly higher than V_{o1_rip} to provide reasonable margin.

TABLE 1 SIMULATED POWER FACTOR PERFORMANCE OF THE PROPOSED LED DRIVER UNDER 110VRMS INPUT

V_{o1_rip} / V_{LED}	5%	10%	20%	30%	40%
Power Factor (V_{aux} = 20V)	0.99	0.98	0.93	0.85	0.7
Power Factor (V_{aux} = 30V)	0.99	0.99	0.96	0.90	0.78
Power Factor (V_{aux} = 40V)	0.99	0.99	0.97	0.92	0.84
Power Factor (V_{aux} = 50V)	0.99	0.99	0.97	0.94	0.88

As shown in TABLE 1, the power factor of the proposed LED driver is reduced when the ripple ratio $Vrip\_vo1 / V_{LED}$ is increased. Under the same ripple ratio, the power factor is improved when V_{aux} is increased from 20V to 50V. The improvement is not obvious when the ripple ratio is low, for example when the ripple ratio V_{o1_rip} / V_{LED} is 5% or 10%. The improvement becomes obvious when the ripple ratio is high. For example, when $V_{o1\_rip} / V_{LED} = 40\%$, the power factor is improved from 0.7 when V_{aux} =20V to 0.88 when V_{aux} = 50V.

In addition to the power factor requirement, IEC61000-3-2 class C sets limit on the input harmonic currents for lighting devices with greater than 75W power. The AC input current during interval II operation contributes to the additional harmonic currents. The input harmonic currents are simulated based on 110Vrms input, 50V, 1.5A, 75W output and the results are presented in Fig. 7.

Fig. 7(a) shows the input harmonic currents with $V_{o1\_rip} / V_{LED} = 5\%$ and $V_{aux} = 20V$. Each order of input harmonic current is well below the limit set by IEC-61000-3-2, class C. Fig. 7(b) shows the input harmonic currents when $V_{o1\_rip} / V_{LED} = 10\%$. Each order of input harmonic current is still below the limit. However, the 21th, 23th order input harmonic currents are already very close to the 3% limit. Fig. 7(c) shows the input harmonic currents when $V_{o1\_rip} / V_{LED} = 20\%$. The input harmonic currents from the second interval input current contribute significantly to the overall harmonic current. As a result, multiple harmonic currents exceed the limit.
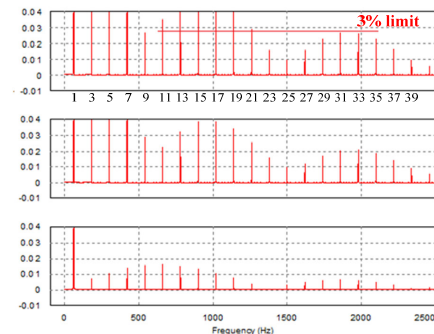
Above simulation results show that the input harmonic currents in Fig. 7(a) and Fig. 7 (b) meet the requirement from IEC-61000-3-2 class C while the input harmonic currents in Fig.7 (c) exceeds the limit. In general, to reduce the input current harmonic currents, it is preferred to have a small V_{o1_rip} / V_{LED}.

3417
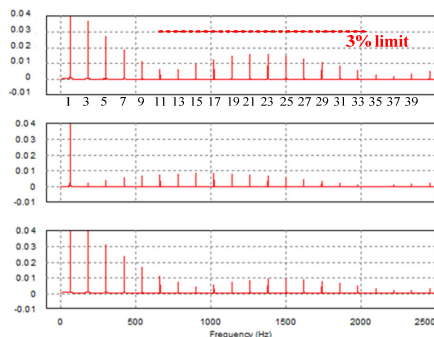
(a) $V_{aux} = 20$, $V_{o1\_rip} / V_{LED} = 5\%$
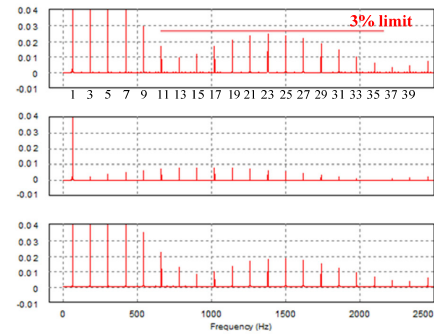
(b) $V_{aux} = 20$, $V_{o1\_rip} / V_{LED} = 10\%$

(c) $V_{aux} = 20$, $V_{o1\_rip} / V_{LED} = 20\%$

Fig. 7 Input harmonic currents when $V_{in} = 110$Vrms, $V_{LED} = 50$V, $I_{LED} = 1.5$A, $V_{aux} = 20$V

V. EXPERIMENTAL VERIFICATIONS

To verify the proposed MRC LED driver, a 7.5W experimental prototype had been designed based on the procedure presented in previous section, built and tested. TABLE 2 gives the design specification and the circuit parameter of the experimental prototype.

TABLE 2 DESIGN SPECIFICATION AND CIRCUIT PARAMETER

Design Specification	
Input Voltage	89Vrms – 132Vrms
V_{LED}	~ 50V
I_{LED}	0.15A
Circuit Parameter	
Coupled inductor	N_1: N_2 = 8:1, L_{N1}=1.25mH EE16 core
Main MOSFET Q_1	2SK2803 (450V 3A)
Main output diode D_1	LQA06T300 (300V 6A)
MOSFET Q_2	ZXMN4A06GTA (40V 5A)

Output diode D_2	MBRS340T3G (40V 4A)
Capacitor C_{aux}	ECA-1HM470B (47µF, 50V)
Output capacitor C_{o1}	EKZE101ELL271MK30S (270µF, 100V)
Output capacitor C_{o2}	CL21A226KOQNNNE (22µF, 16V)
LED current sensing resistor	KNP100JR-73-0R5 (0.5 ohm)
Controller	PIC16F1578-I/SS
Switching frequency f_s	20kHz

Fig. 8 shows the ripple cancellation waveforms of the proposed MRC LED driver. The double-line-frequency ripple voltage on the output V_{o1} is 2V peak to peak. The output V_{o2} generate an opposite ripple voltage to cancel the ripple voltage of V_{o1}. In this way, the double-line-frequency ripple voltage on the LED is greatly reduced. The double-line-frequency ripple LED current is measured to be 16mA peak to peak, which means 20mA peak and the ripple current is 5.3% of the average LED current.
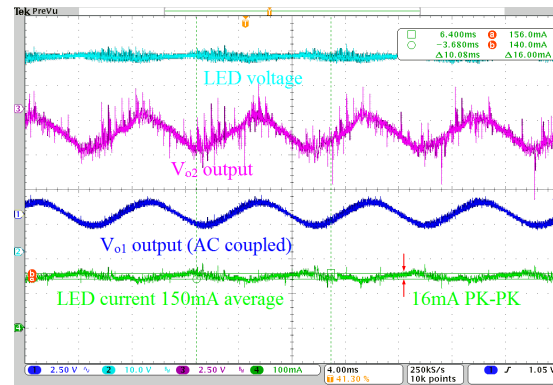

Fig.8 Ripple cancelation waveforms of the proposed MRC LED driver

Fig. 9 shows the gate driving and the switching current waveforms of the MRC LED driver. A switching circle starts at time t0 when the MOSFET Q_1 is turned on. The magnetic current in winding N_1 (and Q_1) starts rising from zero. The magnetic current peaks at t1 when Q_1 is turned off and it continues flowing in D_1. The magnetic current drops to zero before the time t_2, which ends the interval I operation. The MOSFET Q_1 is turned on at t_2 again and the magnetic current in winding N_1 starts increasing from zero again. The current peaks at t_3 when Q_1 is turned off. The magnetic current then commutes from winding N_1 to winding N_2 and continues its flow in diode D_2 and MOSFET Q_2. The current in winding N_2 drops to zero at time t_4, which ends the interval II operation.
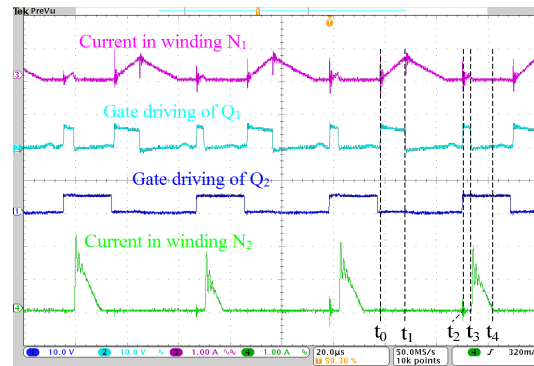

Fig. 9 Key switching waveform of the MRC LED driver

3418

Fig. 10 shows the voltage stresses of Q_1, Q_2 and D_2 in the experimental prototype. The input current waveform and the output voltage waveforms are also included to reflect full load operating condition. The maximum voltage of Q_1 is around 190V. The voltage stresses of Q_1 in the LED driver is the same as it is in a conventional Buck-Boost LED driver. The voltage across the anode of diode D_2 and the source of Q_2 is measured. When the voltage is positive, it indicates D_2 is forward biased while the body diode of Q_2 is reversely biased. Vice versa, it indicates D_2 is reversely biased while the body diode of Q_2 is forward biased. Therefore, as shown from Fig. 10, the maximum voltage on D_2 is around 6V while the maximum voltage on Q_2 is around 20V.
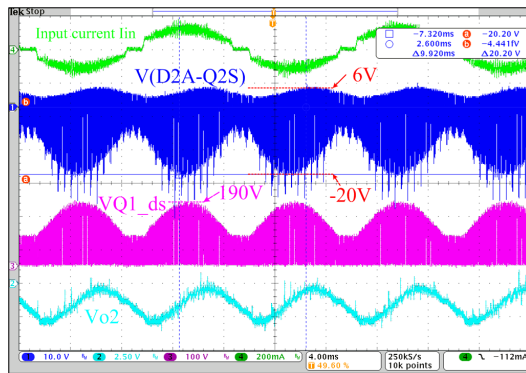

Fig. 10 Power components voltage stresses of the MRC LED driver

Fig. 11 shows the efficiency of the proposed MRC LED driver with and the efficiency of a conventional single-stage Buck-Boost LED driver. The efficiency of MRC prototype is 1% lower than the efficiency of a conventional LED driver. This is due to extra switching loss with the second interval operation. Overall, this is a very small price to pay when flicker-free LED driving performance is achieved. On the other side, to achieve flicker-free LED driving performance and the same efficiency with a two-stage LED driver, the second stage DC-DC converter needs to achieve 99% efficiency, which is not realistic to achieve with a conventional design. Assuming the second stage Buck converter achieves 95% efficiency, the final efficiency of the two-stage LED driver will be 85% x 0.95 = 80.7%, which will be significantly lower than the proposed LED driver.
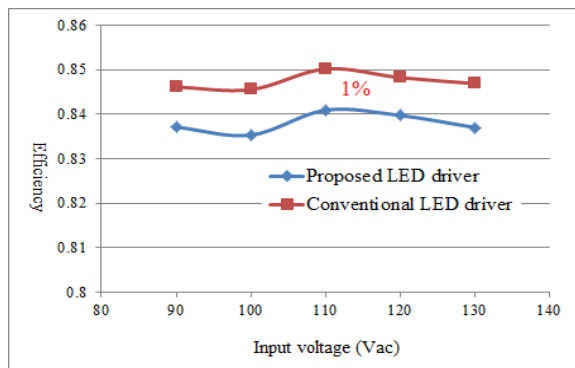

Fig. 11 Efficiency of the experimental prototype LED driver with/without Ripple Cancellation Unit under full load condition

Fig. 12 shows the power factor correction performance of the proposed MRC LED driver. Around 0.98PF has been achieved under full load condition. Fig. 13 shows the input current harmonics of the proposed LED driver. The experimental results show that the converter is able to meet the requirements outlined by IEC 61000 3 2 class C, however, the 9th and 11th order harmonic currents are very close to the limit. It is expected that the input current harmonics can be further reduced with an optimized input filter design.
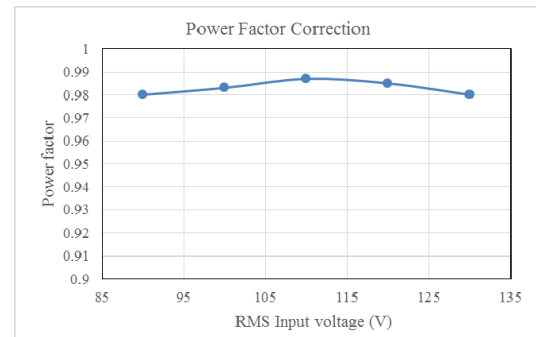

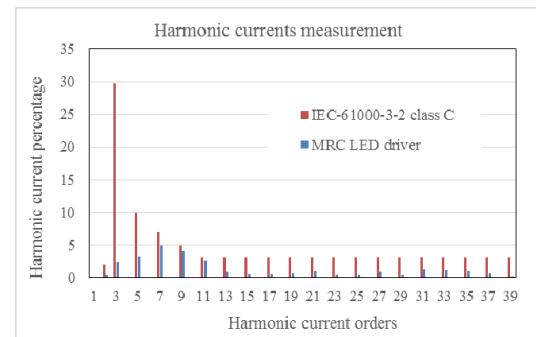Fig. 12 Power Factor Correction performance of the MRC LED driver

Fig. 13 Input current harmonics of the proposed MRC LED driver under 110Vrms input

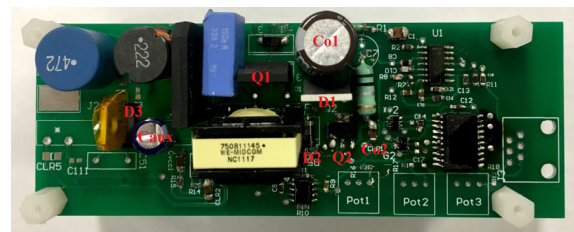Fig. 14 shows the photo of the experimental prototype.

Fig. 14 7.5W MRC LED Driver experimental prototype

VI. CONCLUSION

In this paper, a Multiplexing Ripple Cancellation LED driver is proposed in this paper to achieve flicker-free LED driving, high efficiency and a high power factor correction. The power circuit is operated in time multiplexing manner with two intervals in one switching cycle. The operation in the interval I performs power factor correction and transfers energy from the AC input to the LED load. The operation in the interval II produced the opposite ripple voltage to achieve ripple cancellation. The proposed MRC LED driver also achieves true single-stage power conversion, improving efficiency over previous ripple cancellation LED driver. The

LED driver can maintain a low cost by minimizing additional components, making it a very competitive solution for cost-sensitive low power designs. A 7.5W experimental prototype had been built and tested to verify the operation of the LED driver. The experimental prototype achieves 0.98PF, 5.3% of double-line-frequency ripple LED current performance while the efficiency is only 1% efficiency lower than a conventional Buck-Boost LED driver.

REFERENCES

[1] Global LED Lighting Market Is Set for a Rapid Growth and is Expected to Reach USD 54.28 Billion by 2022. Retrieved Oct 20, 2017, from https://www.zionmarketresearch.com/news/led-lighting-market

[2] ENERGY STAR Program Requirements for Solid State Lighting Luminaires, Version 1.1 , December 19, 2008.

[3] B. Lehman, A.J. Wilkins, "Designing to Mitigate Effects of Flicker in LED Lighting: Reducing risks to health and safety," in IEEE Power Electronics Magazine, Vol 1, No 3, September 2014. pp. 18-26.

[4] S. Wang, X.B. Ruan, K. Yao, S.C. Tan, Y. Yang and Z.H. Ye, "A Flicker-Free Electrolytic Capacitor-Less AC–DC LED Driver" in IEEE Transactions on Power Electronics, Vol. 27, No. 11, pp.4540-4548, November 2012.

[5] Y. Yang, X.B. Ruan, L. Zhang, J.X He and Z.H Ye, "Feed-Forward Scheme for an Electrolytic Capacitor-Less AC/DC LED Driver to Reduce Output Current Ripple," in IEEE Transactions on Power Electronics, Vol. 29, No. 10, pp. 5508-5517, Octorber 2014.

[6] P. T. Krein, R. S. Balog and M. Mirjafari, "Minimum Energy and Capacitance Requirements for Single-Phase Inverters and Rectifiers Using a Ripple Port," in IEEE Transactions on Power Electronics, Vol. 27, No. 11, pp. 4690-4698, November. 2012.

[7] B.B. Wang, X.B. Ruan, K. Yao and M. Xu, "A Method of Reducing the Peak-to-Average Ratio of LED Current for Electrolytic Capacitor-Less AC–DC Drivers," in IEEE Transactions on Power Electronics, Vol. 25, No. 3, pp.592-601, March 2010.

[8] J. C. W. Lam and P. K. Jain, "Isolated AC/DC Offline High Power Factor Single-Switch LED Drivers Without Electrolytic Capacitors," in IEEE Journal of Emerging and Selected Topics in Power Electronics, Vol. 3, No. 3, pp. 679-690, September 2015.

[9] J. C. W. Lam and P. K. Jain, "A High Power Factor, Electrolytic Capacitor-Less AC-Input LED Driver Topology With High Frequency Pulsating Output Current," in IEEE Transactions on Power Electronics, Vol. 30, Vo. 2, pp. 943-955, Feburary 2015.

[10] Z. Bo, Y. Xu, X. Ming, Q.L. Chen and Z.A. Wang, "Design of Boost-Flyback Single-Stage PFC converter for LED power supply without electrolytic capacitor for energy-storage," in International Power Electronics and Motion Control Conference, Wuhan, 2009.

[11] K. M. Divya and R. Parackal, "High power factor integrated buck-boost flyback converter driving multiple outputs," in Online International Conference on Green Engineering and Technologies, Coimbatore, 2015

[12] D. G. Lamar, J. Sebastian, M. Arias and A. Fernandez, "On the Limit of the Output Capacitor Reduction in Power-Factor Correctors by Distorting the Line Input Current," in IEEE Transactions on Power Electronics, Vol. 27, No. 3, pp. 1168-1176, March 2012.

[13] Q.C. Hu and R. Zane, "Minimizing Required Energy Storage in Off-Line LED Drivers Based on Series-Input Converter Modules," in IEEE Transactions on Power Electronics, Vol. 26, No. 10, pp.2887-2895, October 2011.

[14] X.B. Ruan, B.B. Wang, K. Yao and S. Wang, "Optimum Injected Current Harmonics to Minimize Peak-to-Average Ratio of LED Current for Electrolytic Capacitor Less AC–DC Drivers" in IEEE Transactions on Power Electronics, Vol. 26, No. 7, pp.1820-1825, July 2011.

[15] D.Camponogara, D.R.Vargas, M.A.Dalla Costa, J.M.Alonso, J.Garcia and T.Marchesan, "Capacitance reduction with an optimized converter connection applied to LED drivers," in IEEE Transactions on Industrial Electronics, Vol. 62, No.1, pp.184-192, January 2015.

[16] D.Camponogara, G.F.Ferreira, A. Campos, M.A. Dalla Costa and J. Garcia, "Offline LED Driver for Street Lighting With an Optimized Cascade Structure," in IEEE Transactions on Industry Applications, Vol.49, No 6, pp.2437-2443, December 2013.

[17] P. Fang, Y. j. Qiu, H. Wang and Y. F. Liu, "A Single-Stage Primary-Side-Controlled Off-line Flyback LED Driver with Ripple Cancellation," in IEEE Transactions on Power Electronics, Vol. 32, no. 6, pp. 4700-4715, June 2017.

[18] Y. Qiu, L. Wang, H. Wang, Y. F. Liu and P. C. Sen, "Bipolar Ripple Cancellation Method to Achieve Single-Stage Electrolytic-Capacitor-Less High-Power LED Driver," in IEEE Journal of Emerging and Selected Topics in Power Electronics, vol. 3, no. 3, pp. 698-713, Sept. 2015.

[19] P. Fang, Y. F. Liu and P. C. Sen, "A Flicker-Free Single-Stage Offline LED Driver With High Power Factor," in IEEE Journal of Emerging and Selected Topics in Power Electronics, vol. 3, no. 3, pp. 654-665, Sept. 2015.

[20] P. Fang and Y. F. Liu, "Energy Channeling LED Driver Technology to Achieve Flicker-Free Operation with True Single Stage Power Factor Correction," in IEEE Transactions on Power Electronics, vol. 32, no. 5, pp. 3892-3907, May 2017.

[21] Y.C. Li and C.L. Chen, "A Novel Primary-Side Regulation Scheme for Single-Stage High-Power-Factor AC–DC LED Driving Circuit," in IEEE Transactions on Industrial Electronics, Vol. 60, No. 11, pp.4978-4986, November 2013.

[22] X.G. Xie, J. Wang, C. Zhao, Q. Lu and S.R. Liu, "A Novel Output Current Estimation and Regulation Circuit for Primary Side Controlled High Power Factor Single-Stage Flyback LED Driver," in IEEE Transactions on Power Electronics, Vol. 27, No. 11, pp. 4602-4612, November 2012.

[23] H.H. Chou, Y.S. Hwang and J.J. Chen, "An Adaptive Output Current Estimation Circuit for a Primary-Side Controlled LED Driver," IEEE Transactions on Power Electronics, Vol.28, No.10, Oct. 2013, pp.4811,4819

[24] J.M. Zhang, H.L. Zeng and T. Jiang, "A Primary-Side Control Scheme for High-Power-Factor LED Driver With TRIAC Dimming Capability," IEEE Transactions on Power Electronics, Vol.27, No.11, Nov.2012, pp.4619,4629,

[25] C.A. Cheng, C.H. Chang, T.Y. Chung and F.L. Yang, "Design and Implementation of a Single-Stage Driver for Supplying an LED Street-Lighting Module With Power Factor Corrections," in IEEE Transactions on Power Electronics, Vol. 30, No. 2, pp. 956-966, February 2015.

[26] F.H. Zhang, J.J.Ni and Y.J.Yu, "High Power Factor AC–DC LED Driver With Film Capacitors," in IEEE Transactions on Power Electronics, Vol. 28, No. 10, pp. 4831-4840, October 2013.

[27] W. Chen and S.Y.R. Hui, "Elimination of an Electrolytic Capacitor in AC/DC Light-Emitting Diode (LED) Driver With High Input Power Factor and Constant Output Current," in IEEE Transactions on Power Electronics, Vol. 27, No. 3, pp. 1598-1607, March 2012.

[28] H. Ma, J. S. Lai, Q. Feng, W. Yu, C. Zheng and Z. Zhao, "A Novel Valley-Fill SEPIC-Derived Power Supply Without Electrolytic Capacitor for LED Lighting Application," in IEEE Transactions on Power Electronics, Vol. 27, No. 6, pp. 3057-3071, June 2012.

[29] U. Ramanjaneya Reddy and B. L. Narasimharaju, "Single-stage electrolytic capacitor less non-inverting buck-boost PFC based AC–DC ripple free LED driver," in IET Power Electronics, vol. 10, no. 1, pp. 38-46, 2017.

[30] Y.Q. Hu, L. Huber, M.M. Jovanović, "Single-Stage, Universal-Input AC/DC LED Driver With Current-Controlled Variable PFC Boost Inductor," in IEEE Transactions on Power Electronics, Vol. 27, No. 3, pp.1579-1588, March 2012.

[31] Y.C. Li and C.L Chen, "A Novel Single-Stage High-Power-Factor AC-to-DC LED Driving Circuit With Leakage Inductance Energy Recycling," in IEEE Transactions on Industrial Electronics, Vol. 59, No. 2, pp.793-802, February 2012.

[32] R.H. Zhang, H.S. Chung, "A TRIAC-Dimmable LED Lamp Driver With Wide Dimming Range," in IEEE Transactions on Power Electronics, Vol. 29, No. 3, pp. 1434-1446, March 2014.

[33] K. Yao, X. Fu and J. Lv, "DCM Flyback PFC converter with optimum utilization control of switching cycles," *2015 IEEE Energy Conversion Congress and Exposition (ECCE)*, Montreal, QC, 2015, pp. 2445-2452.